ISSN- 0102-9010

ULTRASTRUCTURAL ASPECTS OF THE MUSCLE OF THE ANTERIOR THIRD OF RABBIT TONGUE

Jussara Loli Oliveira[1], Ii-sei Watanabe[1], Koichi Ogawa[2], Aracy Akiko Motoyama[1], Marcelo Cavenaghi Pereira da Silva[1] and Marcia Consentino Kronka[1]

[1]Departament of Anatomy, Institute of Biomedical Sciences, University of São Paulo (USP), São Paulo, SP, Brazil, [2]Departament of Anatomy, School of Medicine, Fukuoka University, Fukuoka, Japan.

ABSTRACT

The structural organization of the anterior third of adult rabbit tongue was studied using light microscopy and conventional and high resolution scanning electron microscopy. Histologically, the muscle layer of the tongue consisted of muscle fibers arranged vertically, transversally and longitudinally. These fibers were surrounded by connective tissue containing bundles of collagen fibers that formed the endomysium and the perimysium. Capillary blood vessels were noted in the connective tissue between muscle fibers. Silver impregnation demonstrated the presence of numerous bundles of nerve fibers distributed irregularly around the muscle fibers. High-resolution scanning electron microscopy showed that the sarcoplasm of the muscle cells consisted of bundles of myofilaments arranged longitudinally and numerous mitochondria.

Key words: Light microscopy, muscle, rabbit, scanning electron microscopy, tongue

INTRODUCTION

In animals with taste buds the tongue has sensorial functions and is also involved in mastication and swallowing, in the arrangement of teeth and in phonation. The tongue consists of extrinsic and intrinsic muscle fibers arranged transversally, vertically and longitudinally [28].

The tongues of several species of animals have been studied, especially the structure and function of the taste buds [10,16,18,25]. More recent work has assessed the usefulness of tongue morphology for classifying animals and for explaining the specialization of the masticatory system. Several investigations using rabbits have examined the embryology, function and the capacity of the tongue to heal and regenerate after surgery [1,8,9,15,17].

In addition to elective surgeries, several esthetic surgical procedures are now common, including piercing the body of the tongue, or bisectioning the tip of the tongue to produce a bifurcated or bifid tongue known as "snake tongue". Since all of these procedures alter the function of the tongue, they also probably affect the ultrastructure of the muscles involved.

Correspondence to: Dr. Ii-sei Watanabe
Departamento de Anatomia, Instituto de Ciências Biomédicas III, Universidade de São Paulo (USP), Av. Prof. Lineu Prestes, 2415, CEP: 05508-900, São Paulo, SP, Brasil. Tel. (55) (11) 3091-7386, Fax: (55) (11) 3091-7366, E-mail: watanabe@icb.usp.br

In this study, we examined the three-dimensional and ultrastructural characteristics of the muscle of the anterior third of rabbit tongues using light microscopy and conventional and high resolution electron microscopy.

MATERIAL AND METHODS

The tongues of eight adult (2-3 Kg) rabbits (*Oryctolagus cuniculus*) of both sexes were used. The rabbits were anesthetized with *i.v.* injection of sodium pentobarbital (30 mg/Kg) and perfused with modified Karnovsky's containing 2.5% glutaraldehyde and 2% paraformaldehyde in 0.1 M sodium phosphate solution (pH 7.4). For scanning electron microscopy, six tongues were fixed in the same solution for 24 h at 4°C and then frozen in liquid nitrogen (-196°C) and fractured with a chisel and hammer. Some specimens were incubated with 10% NaOH solution for 4 to 6 days to digest the soft tissues. Subsequently, all specimens were rinsed in distilled water then postfixed in 1% OsO_4 in 0.1 M sodium phosphate buffer (pH 7.4) for 2 h at 4°C and dehydrated through a graded ethanol series before critical point drying. The specimens were mounted on metal stubs, coated with gold and examined with a JEOL JSM-6100 scanning electron microscope [25].

For routine light microscopy, two tongues were fixed in 10% formalin or Bouin's fixative for 12 h, and then embedded and stained with hematoxylin-eosin, picro-sirius and azo-carmin. To observe the nerve fibers, tongues were fixed in formalin for 20 days at room temperature and sections 40-60 μm thick were cut on a cryostat (Kriostil System Ditts, Duspiva). The specimens were dehydrated, immersed in 20% silver nitrate solution and developed and fixed as described elsewhere [40]. The sections were examined with a Zeiss photomicroscope.

For high-resolution scanning electron microscopy (HRSEM), the samples were prepared using the prefixation osmium-dimethyl sulfoxide (DMSO) method [32-34,39]. The samples were fixed in 2% buffered osmium tetroxide for 2 h at 4°C, rinsed in distilled water and then immersed in 12.5%, 25% and 50% DMSO for 30 min each. The specimens were frozen on a metal plate, chilled with liquid nitrogen and split with a razor blade and a hammer in a freeze-fracture apparatus (TF-1, Eiko Engineering Co. Ltd., Japan). The pieces were placed in 50% DMSO and thawed at room temperature. After post-fixation in 2% osmium tetroxide for 2 h at 4°C and treatment with 1% tannic acid for 2 h at room temperature, the specimens were dried in a critical-point dryer (Eiko ID-2, Japan) then coated with gold-palladium in a BIO-RAD-SEM coating system (Japan) and examined in a high-resolution scanning electron microscope (Hitachi, S-900, Japan).

RESULTS

The epithelial layer of the tongue consisted of a stratified keratinized epithelium with superficial

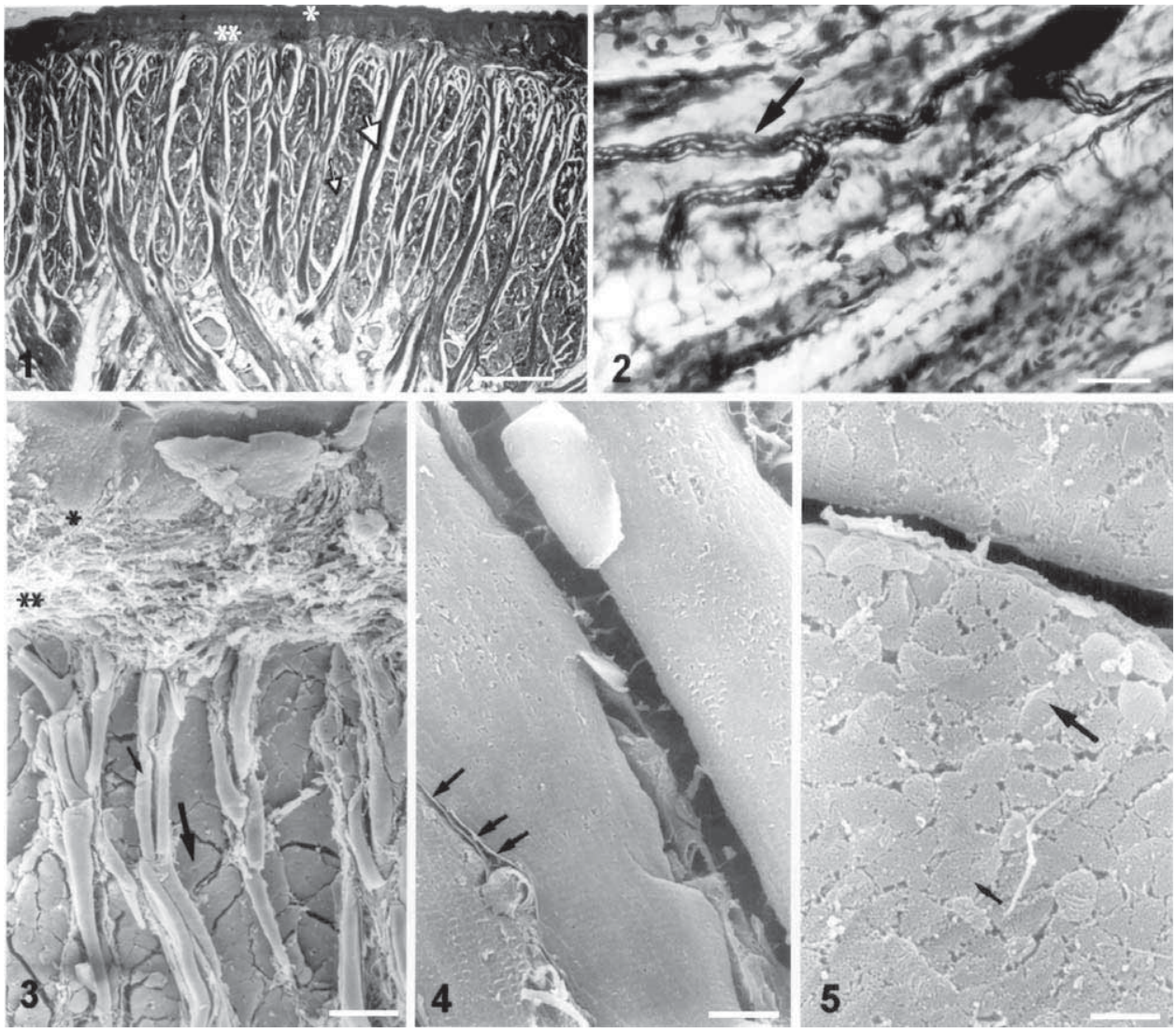

Figure 1. Light photomicrograph showing the general aspect of the anterior third of a rabbit tongue with epithelium (*), connective tissue (**), and muscle fibers sectioned longitudinally (**large arrow**) and transversely (**small arrow**). Bar = 550 µm.
Figure 2. Silver impregnation showing the sparsely distributed nerve bundles (arrow). Bar = 50 µm.
Figure 3. General aspect of a fractured specimen showing the basal layer of the epithelium (*), the connective tissue (**), and muscle fibers disposed longitudinally (**small arrow**) and sectioned transversely (**large arrow**). Bar = 80 µm.
Figure 4. SEM of a longitudinally fractured specimen showing the sarcoplasmic membrane of a muscle fiber in the anterior third of the tongue. The **arrows** indicate the endomysium. Bar = 10µm.
Figure 5. High resolution SEM showing mitochondria (**large arrow**) and myofilaments (**small arrow**). Bar = 1 µm.

squamous cells, connective tissue underneath and muscle fibers arranged in several directions (Fig. 1). The connective tissue surrounding the muscle bundles formed the perimysium while the thin layer involving each muscle fiber formed the endomysium. Treatment of the samples with NaOH revealed bundles of nerve fibers arranged in various directions and irregular and short tortuous isolated nerve fibers at the periphery of the muscle fiber (Fig. 2). Electron microscopy showed that the connective tissue was closely applied to epithelial cells of the basal layer and also to muscle fibers (Figs. 3 and 7).

Capillaries and dense bundles of collagen fibers were seen in the connective tissue. The muscle layer consisted of fibers arranged in many directions. The vertical fibers were inserted at different levels and were 8 to 12 μm in diameter, as shown by high magnifications of transversal sections. Fracturing revealed intracellular components and the sarcoplasmic membrane (Fig. 4), as well as capillaries and collagen fibers at the periphery. These collagen fibers formed the endomysium and groups of muscle fibers formed the fasciculi which were surrounded by more substantial collagen bundles constituting the perimysium.

Mitochondria were observed among the myofilaments (Fig. 5), and their cristae were visible at higher magnification (Fig. 6). Round or oval mitochondria arranged in series and myofilaments arranged longitudinally were seen in longitudinal fractures (Fig. 8).

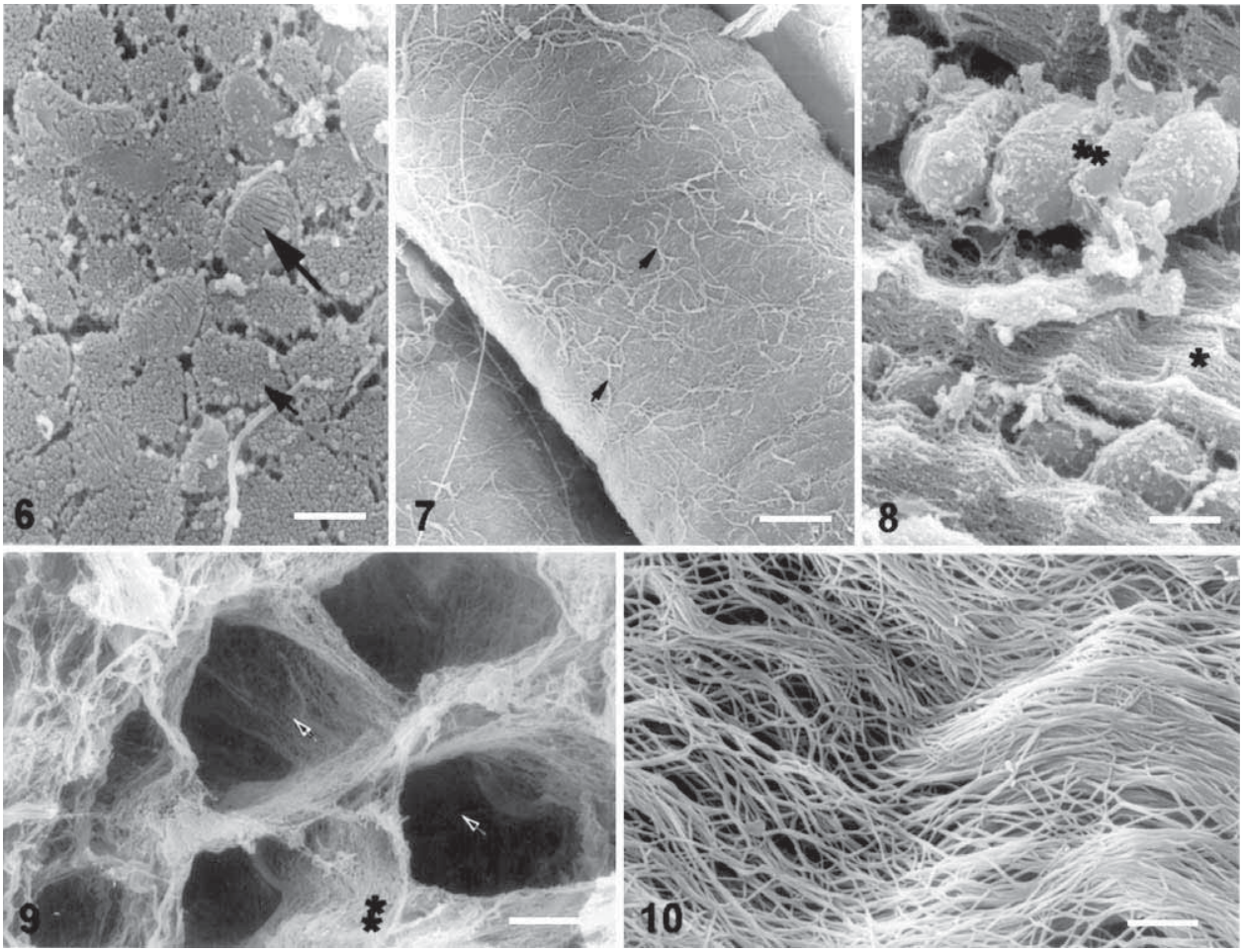

Figure 6. High resolution SEM showing mitochondria (**large arrow**) and myofilaments (**small arrow**). Bar = 560 nm.
Figure 7. Electronmicrograph showing the surface of a muscle fiber with several collagen fibers (**arrows**). Bar = 3.7 μm.
Figure 8. Electronmicrograph showing a fractured muscle fiber with myofilaments arranged longitudinally (*) and a series of oval mitochondria (**). Bar = 700 nm.
Figure 9. Specimen treated with a 10% NaOH solution. Note the honeycomb aspect formed by the endomysium (**) around the spaces left by the absent muscle fibers (**arrows**). Bar = 3.8 μm.
Figure 10. The structural arrangement of collagen fibers of the endomysium. Bar = 1 μm.

In specimens treated with 10% NaOH, the spaces occupied originally by muscle fibers were visible (Fig. 9). The collagen network of this region of the tongue had a honeycomb appearance, with bundles of collagen fibers visible at higher magnification (Fig. 10).

DISCUSSION

Carpentier and Pajoni [3] reported that the organization of the tongue muscular layer was similar in mammals. Our findings using high resolution scanning electron microscopy support this conclusion since muscle fibers arranged in various directions have also been reported in primate [11,12,38], human [2,13] and rat [31] tongues. Round or oval mitochondria were observed among myofilaments in the sarcoplasm of the muscle fibers, as also reported for skeletal muscle [22-24,27,30,34,39]. In addition, the myofilaments were arranged longitudinally in the muscle fibers, as previously reported [26,35].

High resolution scanning electron microscopy showed that the ultrastructure and three-dimensional organization of the muscle fibers, connective tissue and blood vessels of the rabbit tongue were similar to those of the corresponding region of the rat and dog tongues studied using a similar approach [10,16]. In the latter case, a vascular region with arteries was seen deep within the muscular layer and there were coiled capillaries in the connective tissue of the endomysium.

The arrangement of the connective tissue in tongue muscle, with small holes for the passage of blood vessels and nerves that made up the epimysium, perimysium and endomysium, has also been reported for other species [14,19,25,35].

Treatment with sodium hydroxide solution showed that the internal surface of the network of collagen fibers had a honeycomb appearance, as also described elsewhere [19,37]. As previously reported for paravertebral musculature in rats [35], this organization of the collagen fibers of the endomysium in the tongue may have a role in preventing the rupture of muscle fibers during contraction. Although high resolution scanning electron microscopy has shown the organization of endomysium collagen fibers into a three-dimensional network outside the basal lamina [10], little was known about the relationship of muscle fiber to collagen fibers, such as observed here.

The pattern of muscle innervation varies according to the sample and type of muscle fiber [21,36]. The presence of several scattered bundles of nerve fibers throughout the muscle layer and the presence of nerve endings in different types of muscle fibers agreed with previous reports [4,5,7,20,29,38]. Some isolated nerve fibers similar to those previously described [6,21] were also seen.

REFERENCES

1. Aeba H, Yamamura K, Inoue M, Hanada K, Ariyasinghe S, Yamada Y (2002) Effects of the inferior alveolar nerve stimulation on tongue muscle activity during mastication in freely behaving rabbits. *Brain Res.* **956**, 149-155.
2. Bell WA (1970) Muscle patterns of the late fetal tongue tip. *Angle Orthod.* **40,** 262-265.
3. Carpentier P, Pajoni D (1989) La lingua: un insiene muscolare complesso. *Mondo Ortod.* **14,** 765-773.
4. Cecio A, Avitabile G, Langella M (1984) Innervation pattern of intrinsic laryngeal musculature of the rabbit. *Acta Anat*. **120,** 234-239.
5. Ezure H (1996) Development of the motor endplates in the masseter muscle in the human fetus. *Anat. Anz.* **178,** 15-23.
6. Feindel W, Hinsshaw JR, Weddel G (1952) The pattern of motor innervation in mammalian striated muscle. *J. Anat*. **86,** 35-48.
7. Freije J, Malmgren LT, Gacek RR (1987) Motor end-plate distribution in the human interarytenoid muscle. *Arch. Otolaryngol. Head Neck Surg*. **113,** 63-68.
8. Fujimoto S, Yamamoto K, Yoshizuka M, Yokoyama M (1993) Pre- and postnatal development of rabbit foliate papillae with special reference to foliate gutter formation and taste bud and serous gland differentiation. *Microsc. Res. Tech*. **26**, 120-132.
9. Greene CH, Debias DA, Henderson MJ, Fair-Covely R, Dorf B, Radin AL, Young-Seidman WL (1994) Healing of incisions in the tongue: a comparison of results with milliwatt carbon dioxide laser tissue welding versus suture repair. *Ann. Otol. Rhinol. Laryngol*. **103**, 964-974.
10. Kishi Y, So S, Harada Y, Takahashi K (1988) Three-dimensional SEM study of arterio-venous anastomoses in the dog's tongue using corrosive resin casts. *Acta Anat*. **132,** 17-27.
11. Kubota T, Hayama S (1964) Comparative anatomical and neurohistological observations on the tongues of pigmy and commom marmosets. *Anat. Rec*. **150,** 473-485.
12. Kubota K, Iwamoto M (1967) Comparative anatomical and neurohistological observations on the tongue of slow loris (*Nycticebus coucang*). *Anat. Rec*. **158,** 163-175.
13. Kubota K, Negishi T, Masegi T (1975) Topological distribution of muscle spindles in the human tongue and its significance in proprioception. *Bull. Tokyo Med. Dent. Univ.* **22,** 235-242.
14. Macconnachie HF, Enesco M, Leblond CP (1964) The mode of increase in the number of skeletal muscle nuclei in the postnatal rat. *Am. J. Anat*. **114,** 245-253.
15. Mameli O, Melis F, Caria MA, Podda MV, Solinas A, Becciu A, De Riu PL (1995) Olfactory influence on tongue activity. *Arch. Ital. Biol.* **133,** 273-288.
16. Motoyama AA, Watanabe I (2001) Light and scanning electron microscopic studies of the angioarchitecture of intrinsic muscle fibers of the anterior rat tongue. *J. Oral Sci.* **43,** 269-275.
17. Naganuma K, Inoue M, Yamamura K, Hanada K, Yamada Y (2001) Tongue and jaw muscle activities during chewing and swallowing in freely behaving rabbits. *Brain Res.* **915**, 185-194.

18. Nakamura M, Okada S (1992) Microvascular architecture of lingual papillae in the Japanese monkey (*Macaca fuscata fuscata*). *Okajimas Folia Anat. Jpn*. **69,** 183-197.
19. Nishimura T, Hattori A, Takahashi K (1994) Ultrastructure of the intramuscular connective tissue in bovine skeletal muscle. A demonstration using the cell-maceration/scanning electron microscope method. *Acta Anat*. **151,** 250-257.
20. Oda K, Shibasaki H (1988) Antigenic difference of acetylcholine receptor between single and multiple form endplates of human extraocular muscle. *Brain Res*. **449,** 337-340.
21. Ogata T (1988) Structure of motor endplates in the different fiber types of vertebrate skeletal muscles. *Arch. Histol. Cytol*. **51,** 385-424.
22. Ogata T, Yamasaki Y (1985) Scanning electron-microscopic studies on the three-dimensional structure of mitochondria in the mammalian red, white and intermediate muscle fibers. *Cell Tissue Res.* **241,** 251-256.
23. Ogata T, Yamasaki Y (1987) High-resolution scanning electron-microscopic studies on the three-dimensional structure of mitochondria and sarcoplasmic reticulum in the different twitch muscle fibers on the frog. *Cell Tissue Res*. **250,** 489-497.
24. Ogata T, Yamasaki Y (1992) Ultra-high-resolution scanning electron microscopic studies on the sarcoplasmic reticulum and mitochondria of the rat intrafusal muscle fibers. Part II: The extracapsular region. *Arch. Histol. Cytol*. **55,** 117-124.
25. Ohtani O, Ushiki T, Taguchi T, Kikuta A (1988) Collagen fibrillar networks as skeletal frameworks: a demonstration by cell-maceration/scanning electron microscope method. *Arch. Histol. Cytol*. **51,** 249-261.
26. Peachey LD, Huxley AF (1962) Structural identification of twitch and slow striated muscle fibers of the frog. *J. Cell Biol.* **13,** 177-180.
27. Rambourg A, Segretain D (1980) Three-dimensional electron microscopy of mitochondria and endoplasmic reticulum in the red muscle fiber of the rat diaphragm. *Anat. Rec*. **197,** 33-48.
28. Sato M, Sato T (1992) Fine structure of developed human tongue muscle. *Okajimas Folia Anat. Jpn*. **69,** 115-130.
29. Sato I, Shimada K, Ezure H, Murakami G, Sato T (1994) Morphological study of nerve endings in jaw muscles of post-hatching American alligators (*Alligator mississippiensis*). *J. Morphol*. **219,** 285-295.
30. Schiaffino S, Hanzlikova V, Pierobon S (1970) Relations between structure and function in rat skeletal muscle fibers. *J. Cell Biol*. **47,** 107-119.
31. Smith KK (1989) Histological demonstration of muscle spindles in the tongue of the rat. *Arch. Oral Biol*. **34,** 529-534.
32. Tanaka K (1980) Scanning electron microscopy of intracellular structures. *Int. Rev. Cytol*. **68,** 97-125.
33. Tanaka K (1981) Demonstration of intracellular structures by high resolution scanning electron microscopy. *Scan. Electron Microsc.* **2***,* 1-8.
34. Tanaka K (1989) High resolution scanning electron microscopy of the cell. *Biol. Cell*. **65,** 89-98.
35. Vasilev V, Andreev D, Kuhnel W (1995) Scanning electron microscopy of the endomysial collagen in the rat paravertebral musculature. *Anat. Anz.* **177,** 85-87.
36. Waerhaug O (1992) Species specific morphology of mammalian motor nerve terminals. *Anat. Embryol*. **185,** 125-130.
37. Watanabe I (1982) Ultra-estrutura da terminação nervosa motora do músculo masseter de camundongos. *Odont. Muscle* **9,** 22-24.
38. Watanabe I, Konig Jr B (1977) Neurohistological observations of the tongue of the tufted capuchin, *Cebus apella* Linnaeus, 1758. *Rev. Bras. Pesqui. Med. Biol*. **10,** 121-127.
39. Watanabe I, Koriyama Y, Yamada E (1992) High-resolution scanning electron microscopic study of the mouse sub-mandibular salivary gland. *Acta Anat*.**143,** 59-66.
40. Winkelman RK, Schimit RW (1957) A simple silver method for nerve axoplasm. *Proc. Staff. Meet Mayo Clin*. **32,** 217-222.

Received: August 23, 2002
Accepted: September 9, 2003